Energy and AI 24 (2026) 100752

Contents lists available at ScienceDirect

Energy and AI

journal homepage: www.sciencedirect.com/journal/energy-and-ai

Data-driven landscape scenicness mapping for continental-scale onshore wind resource assessment

Ruihong Chen [a,*], Tristan Pelser [b,c], Alena Lohrmann [a,d], Jann Michael Weinand [b], Russell McKenna [a,e]

[a] Chair of Energy Systems Analysis, Department of Mechanical and Process Engineering, ETH Zürich, Zürich, 8092, Switzerland
[b] Institute of Climate and Energy Systems - Jülich Systems Analysis (ICE-2), Forschungszentrum Jülich GmbH, Jülich, 52425, Germany
[c] Chair for Fuel Cells, RWTH Aachen University, Aachen, 52062, Germany
[d] Iceland School of Energy, Reykjavik University, Menntavegur 1, 102 Reykjavik, Iceland
[e] Laboratory for Energy System Analysis, Centers for Nuclear Engineering and Sciences & Energy and Environment, PSI, Villigen, 5232, Switzerland

HIGHLIGHTS

- A machine learning model classifies European scenicness with a high accuracy.
- Land cover category and naturalness are the most important predictors.
- Scenic-area preservation cuts technical potential by 43% with minor cost impact.
- Stricter landscape preservation shifts Europe's main onshore wind producers.

GRAPHICAL ABSTRACT

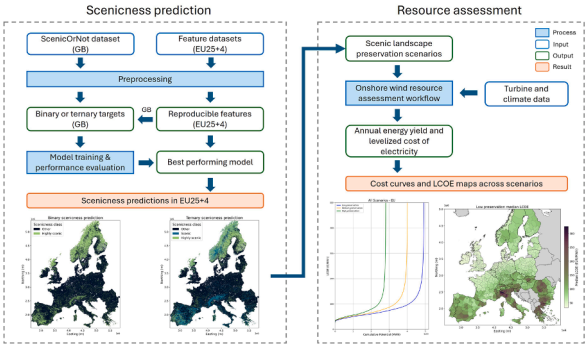

ARTICLE INFO

Keywords:
Machine learning
Classification
Wind energy
Resource assessment
Landscape impacts
Social impacts

ABSTRACT

Visual impacts on scenic landscapes dominate public opposition to onshore wind turbines. Yet wind resource assessments often overlook landscape scenicness due to limited data availability. This study introduces a scalable machine learning framework for generating continental scenicness layers, trained on crowdsourced scenicness ratings from Great Britain and achieving high predictive performance. The resulting scenicness maps are integrated into an onshore wind resource assessment under three landscape preservation scenarios across 29 European countries. We show that prioritizing scenic landscapes in planning can reduce wind generation potential in certain countries by over 60%. However, it only modestly affects the continental median levelized costs of electricity (57 €/MWh and 54 €/MWh under low and high preservation scenarios), while substantially increasing regional costs in scenic mountainous regions such as the Alps and Norway. These findings demonstrate how data-driven approaches can enable socially aware and large-scale energy system planning.

* Corresponding author.
E-mail address: ruchen@ethz.ch (R. Chen).

https://doi.org/10.1016/j.egyai.2026.100752

Available online 14 April 2026

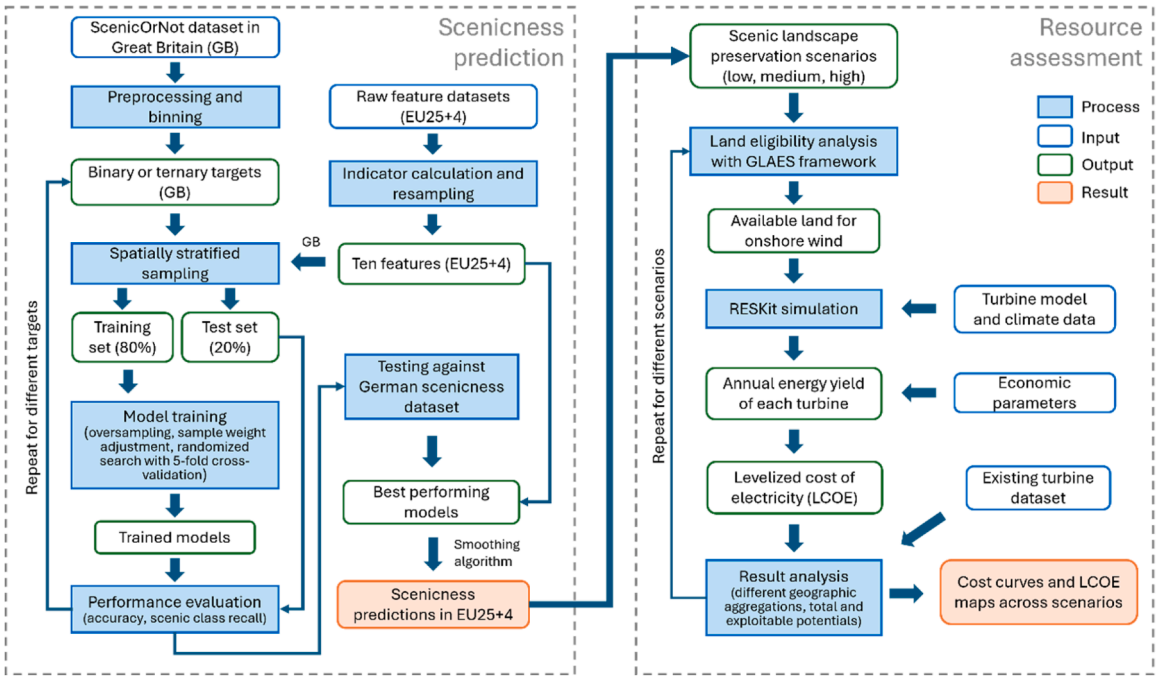

Fig. 1. Overview of methodology for predicting scenicness ratings as well as their usage as scenarios in onshore wind resource assessments with Geospatial Land Availability for Energy Systems (GLAES) [26] and Renewable Energy Simulation Toolkit (RESKit) [27].

1. Introduction

As one of the fastest-growing renewable technologies worldwide, wind energy plays a vital role in the energy transition [1], resulting from its decreasing costs [2], ease of deployment at multiple scales [3], and strong policy support in many countries [4]. Whilst wind energy has a high technology readiness level and cost-competitiveness [2], its large-scale deployment often encounters practical challenges. Especially onshore wind farms face more local opposition than other renewable technologies due to concerns over disruption of scenic landscape, noise emissions, shadow flicker, and effects on wildlife [5]. Still many wind resource assessments overestimate the practical potential of wind deployment by assuming that turbines can be placed wherever technically, economically, and regulatorily feasible [6]. These assessments frequently overlook non-technical constraints [7], especially those stemming from social acceptance and environmental considerations.

In the United Kingdom, for instance, only 42.5% of all onshore wind project applications between 2001 and 2024 have been approved [8], with year-to-year fluctuations due to changes in the energy-political landscape. Even higher local resistance can be observed in Sweden, where 80% of applications were rejected by municipalities in 2021 [9]. Among various perceived impacts of wind farms, visual disturbance of scenic landscapes remains one of the leading causes of opposition [10,11]. People generally oppose wind farms in areas of high natural and scenic value [12,13]. But excluding such areas from development may reduce technical potential and increase total system costs [14,15], implying one of many compromises in the energy domain.

This trade-off between preserving scenic landscapes and expanding wind power highlights a fundamental tension between cost-efficiency and social acceptance. Due to the limited availability of large-scale, high-resolution scenicness ratings, the implications of this trade-off have so far only been quantified for individual case studies in Germany [15–17] and Great Britain [10,14,18]. As wind energy needs to scale up across Europe to meet the 2030 targets [19], a consistent and high-resolution dataset on landscape scenicness is essential to systematically analyze these trade-offs. To date, efforts to model landscape scenicness have shown promise but face significant limitations in scalability. Several studies have used machine learning (ML) to predict scenicness by training models on images [20,21] or survey data [22] on a regional or national scale. While these methods demonstrate the value of data-driven scenicness prediction, their reliance on large collections of photographs or region-specific surveys limits their scalability to larger regions and transferability to different contexts.

To overcome these limitations, we explore how landscape characteristics can relate to scenicness ratings and thereby generate a consistent dataset across Europe. We present a scalable and reproducible ML-based scenicness prediction model using methodological insights from existing landscape literature. Specifically, we utilize the link between landscape patterns and perceived aesthetic value [23] to inform the feature design and adapt the landscape wilderness framework [24] to produce geospatial indicators across Europe. By leveraging a high-resolution national scenicness dataset from Great Britain (ScenicOrNot) [25] and widely available spatial data on land use, topography, infrastructure, and population, our method enables consistent scenicness mapping on a continental-scale for the first time.

Based on the scenicness predictions, we identify areas where wind farms may face greater landscape-based opposition, which is directly applicable to strategic energy planning and modelling at multiple scales. For this, we techno-economically assess the onshore wind potential across Europe, with extensive land use constraints to model the available area, installable capacity and annual energy yield. These outputs serve as invaluable inputs to whole energy system models and can inform policymakers of the likely cost effects of incorporating comprehensive social barriers to wind farm development.

2. Methodology

This section outlines the methodology for training the ML model to predict landscape scenicness across Europe (Section 2.1 – 2.3) and the approach for onshore wind resource assessment (Section 2.4). The ML model outputs are subsequently used to define different landscape preservation scenarios for the resource assessment (see Fig. 1). The geographic scope for the analysis covers **EU25+4** (EU27 excluding Malta and Cyprus but including the United Kingdom, Norway, Switzerland, and Liechtenstein), as determined by data availability.

2.1. Data collection and preprocessing

ML models are trained on existing data, however, to the authors' knowledge, only two national-level landscape scenicness datasets with 1 km^2 spatial resolution are publicly available in Europe, namely the crowd-sourced ScenicOrNot dataset for Great Britain (GB) [25] and an empirically modelled scenicness map for Germany [22].

ScenicOrNot is based on public ratings from 1 (low) to 10 (high) of randomly presented, geo-tagged eye-level photographs, with approximately 212,000 images covering the whole of GB. Its crowd-sourced nature offers a broad representation of perceived scenic quality but includes potential bias from unknown rater demographics. In comparison, the German dataset [22] is based on a model calibrated with a limited public survey on a selection of around 800 photographs, and therefore represents a more indirect estimate of visual quality. Given its size, spatial coverage, and direct public input, ScenicOrNot is selected as the training dataset, while the German dataset is used exclusively for comparison with the trained model's predictions.

In this study, *scenicness* refers to a broad consensus on visual aesthetics based on observable landscape features such as natural vegetation, waterbodies, and topography, attributes that tend to elicit broad public agreement [28]. It is conceptually distinct from place attachment, which reflects personal or cultural ties to a specific location and varies considerably across individuals [29,30]. Focusing on scenicness enables the use of a more generalizable proxy for perceived visual impact in large-scale wind energy planning.

Using the ScenicOrNot dataset, we assume that each image represents the scenery of the surrounding 1 km^2 area, since the direction of each photograph is unknown. As the photographs were shown to online participants randomly, the influence of place attachment is expected to be minimal compared to local surveys [31].

Initial analysis of the dataset revealed that while most locations showed high agreement among raters (variance < 5), around 12% still exhibited high disagreement (variance ≥ 5) (see Figure A 1c in Supplementary Material). This high variance reflects the noise inherent in subjective ratings. To reduce this noise, an iterative outlier-removal procedure was applied. For each point with high variance, the rating furthest from the mean was removed and then mean and variance were recalculated. This process was repeated until the variance fell below a threshold of 5 or until only two ratings remained. Post-processed cases still exceeding the variance threshold were deemed controversial and excluded from training. Lower and more clustered variances in ratings after processing can be observed, indicating less noise (see Figure A 1d in Supplementary Material).

Despite denoising, the scenicness ratings remained left-skewed, with the majority of values falling in the low-to-mid range (see Figure A 1a,b in Supplementary Material). This skewness poses challenges for regression-based models, which may underperform on underrepresented extreme values [32]. To address this, we formulated the prediction task as a classification problem, applying various techniques to handle imbalanced distributions [33,34] and yielding outputs that are more interpretable in the planning context.

Classification thresholds were defined to create binary and ternary labels using a range of cut-off values (see Fig. 4c). Binary targets separated the data into two classes, whereas ternary targets introduced an intermediate class, with the interpretation of each class depending on the chosen thresholds. These thresholds were iteratively adjusted to assess sensitivity of model performance, and the resulting metrics were compared to identify the most informative class splits.

2.2. Feature data and calculation

To train the model, ten predictor variables (features) were selected based on literature review and data availability, reflecting their relevance to perceived landscape scenicness. The first four are landscape wilderness indicators: naturalness, ruggedness, remoteness, and human impact, calculated in this study based on the wilderness framework [24] following the link between wilderness and landscape aesthetics [23]. The methods for calculating these indicators were adapted using European data to ensure reproducibility across the continent. To enhance the model's predictive accuracy and potentially capture the complex relationship between scenicness and geospatial features, six additional features were integrated into the model. An overview of all the features, including their spatial resolutions, units, variable type, and sources, is provided in Table 1.

Table 1
Overview of features used in the machine learning model, including their spatial resolution, unit, variable type and source.

Feature	Spatial resolution	Unit	Variable type	Source
Naturalness	100 m × 100 m	N/A	Discrete	Calculated based on [24,35,36]
Ruggedness	100 m × 100 m	meters	Continuous	Calculated based on [24,36]
Remoteness	100 m × 100 m	minutes	Continuous	Calculated based on [24,35,36]
Human impact	100 m × 100 m	N/A	Continuous	Calculated based on [24,37]
Waterbody proximity	100 m × 100 m	meters	Continuous	[35,37]
Slope aspect angle	100 m × 100 m	degrees (°)	Continuous	[36,37]
Global horizontal irradiance (GHI)	200 m × 200 m	kWh/m^2/year	Continuous	[38,39]
Population density	100 m × 100 m	Inhabitants per hectare	Continuous	[40]
Elevation	90 m × 90 m	meters	Continuous	[36]
CORINE Land cover (CLC)	100 m × 100 m	N/A	Discrete	[35]

During model training, feature values were sampled at their original resolution to preserve raw data accuracy. For predictions on unseen data in other countries, all features were resampled and aligned to a common 1 km^2 grid using average or nearest-neighbor interpolation, depending on whether the data is continuous or discrete.

2.2.1. Wilderness indicators

Naturalness. The naturalness index follows the hemeroby framework [24], which classifies land based on human influence. CLC data [35] were re-classified into a 5-point hemeroby scale (1 = natural, 5 = highly modified) and adjusted for elevation using Copernicus digital elevation model (COP-DEM) data [36]. For certain land cover types found above 1800 m elevation, a lower hemeroby value was assigned to reflect environmental constraints. The full list of land cover classes and their assigned hemeroby indices can be found in Table A 2 in Supplementary Material, providing ordinal information on land covers.

Ruggedness. Ruggedness was quantified as the standard deviation of elevation within a 500 m × 500 m moving window using COP-DEM (90 m × 90 m resolution) [36], which captures terrain complexity and visual depth in landscape perception.

Remoteness. Remoteness was calculated as the estimated walking time from each location to the nearest road from OpenStreetMap (OSM) [41] using a K-dimensional tree (KDTree) search [42] and the Bresenham Line Algorithm [43]. Travel time was derived from the empirical walking speed data [24] for different slopes [36] and land covers [35], the details of which are shown in Table A 3 in Supplementary Material.

Human impact. The human impact indicator aggregates the presence of infrastructures from the Pre-computed Land Indication (PRIOR)

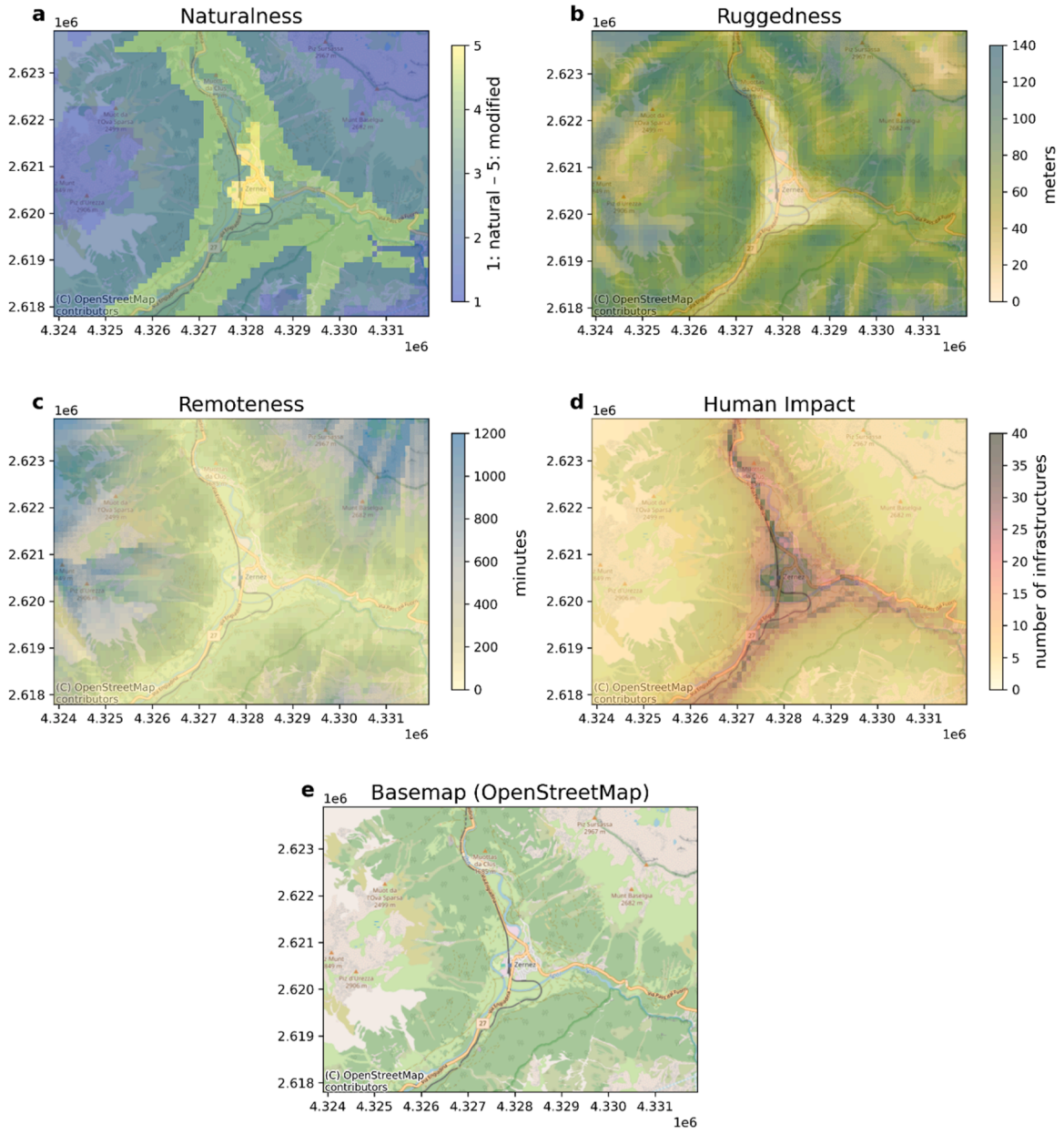

Fig. 2. An illustrative example of the calculated indicators at a village (Zernez) in Switzerland surrounded by mountains with roads and a railway passing through: (a) Naturalness, (b) Ruggedness, (c) Remoteness, (d) Human impact, (e) the basemap from OpenStreetMap.

datasets [37], including agriculture, airports, airfields, camping facilities, industrial areas, settlements, mining sites, leisure facilities, power lines, railways, and roads. Each infrastructure type contributes to the score according to its proximity, modeled through an inverse distance decay function to prevent abrupt discontinuities between adjacent pixels.

An illustrative example of these four calculated indicators for a mountain village in Switzerland is shown in Fig. 2a-e. Each indicator captures a distinct dimension of the landscape, highlighting variations in naturalness ranking, terrain complexity, accessibility, and human activities.

2.2.2. Additional features

As shown in Table 1, six additional features from open-access data were incorporated into the model. The presence of waterbodies, land use types, and elevation are often considered relevant variables in landscape beauty [44,45]. Solar irradiation and slope aspect angles can indirectly shape scenic perception by affecting visual exposure and vegetation patterns [46,47]. Moreover, population density reflects human activities, potentially altering the land use. Accordingly, the six environmental and anthropogenic variables integrated into the model are: proximity to inland waterbodies, annual mean global horizontal irradiance (GHI), population density, CLC, elevation, and slope aspect angle. GHI data were sourced from the Global Solar Atlas [38] (200 m × 200 m resolution), with gaps in northern Europe (above 65° N) filled using PVGIS-SARAH-2 [39] (4.5 km × 4.5 km resolution).

2.3. Model setup, training and testing

The consolidated dataset of classified scenicness and geospatial features was split into training (80%) and test (20%) subsets. Model training and prediction were restricted to non-urban land (excluding water surfaces), as wind farms are rarely located in dense urban settings [48]. Urban areas were identified using urban clusters from EuroStat in

2011 [49], as compiled by PRIOR [37].

Given the imbalanced class distribution and the need to identify highly scenic areas reliably, we selected Extreme Gradient Boosting (XGB) as the primary classifier [50]. XGB offers strong performance with imbalanced data [51,52], interpretable feature importance [53], and robustness to multicollinearity [54] and unscaled inputs [50]. A Logistic Regression (LR) model was simultaneously trained as a benchmark.

The performance metrics for classification tasks include accuracy, recall, precision, and F1-score, all derived from the confusion matrix (see Table B 1 in Supplementary Material). In particular, recall for the highly scenic class measures the proportion of actual scenic locations correctly identified. It was prioritized over precision, as missing scenic areas (false negatives) carries greater consequences for wind energy planning than overestimating them (false positives). To reflect the priority of the highly scenic class, sample weights were set to 2 for the highly scenic class and 0.5 for others.

Because ScenicOrNot data exhibits moderate spatial autocorrelation [55,56] (Moran's I =0.35, $p < 0.05$), we used spatially stratified sampling to mitigate geographically biased training. Specifically, K-Means clustering grouped ScenicOrNot points into spatial clusters of 10,000 based on coordinates, within which class-stratified splits were performed to preserve class distribution across subsets. Training and test sets were then compiled by merging the splits across clusters. For target variables with less than 20% minority class share [57], we applied Synthetic Minority Over-sampling Technique (SMOTE) [58] to the training data after the split to improve performance on underrepresented classes. It should be noted that SMOTE operates in feature space and does not explicitly preserve spatial structure, which may distort local spatial patterns. However, the performance evaluation remains unbiased since no synthetic samples were introduced to the test set. As the primary objective is to develop a transferable model for continental-scale application instead of assessing spatial generalization within GB, spatial cross-validation was not implemented.

Hyperparameters were tuned using randomized search over 10 iterations, optimizing the highly scenic class F1-score in 5-fold cross-validation. The parameter space included number of estimators, learning rate, tree depth, subsample ratio, and regularization terms (see Table B 2 in Supplementary Material). Feature importance scores from the trained models were used to identify the most influential predictors.

The top-performing models in terms of accuracy and highly scenic class recall were first applied to Germany for testing on unseen data, allowing the comparison with the empirically-based modelling outputs [22]. The binary and ternary models showing the highest accuracy were then used to predict scenicness across EU25+4 countries using feature raster data resampled to a 1 km^2 grid. Installed wind turbine data [59] were used to assess whether past siting decisions align with areas predicted as the lower class.

To enhance spatial coherence and reduce false negatives in the final maps, we applied a smoothing algorithm: for each cell predicted as the lowest class, the classes of the four adjacent cells were examined. If a clear majority existed, the focal cell was reassigned to that class; if multiple modes were present, the higher-class value was chosen (see Figure B3 in Supplementary Material). This post-processing step reduces local noise and better reflects the observed clustering of scenic landscapes [60]. Importantly, the smoothing procedure was applied only to the final raster outputs. Its impact was assessed by comparing raw and smoothed raster predictions at the original point locations in GB, enabling a consistent evaluation against the reference scenicness data.

2.4. Scenario development and wind potential calculation

The predicted scenicness classifications were subsequently integrated into a scenario-based assessment of onshore wind potential and costs across Europe using the Renewable Energy Simulation toolkit (RESKit) modelling framework [27]. The analysis explored trade-offs between wind power cost-efficiency and scenic landscape preservation. To enable more granular comparison, the ternary predictions were used to define three exclusion scenarios, which were combined with the standardized European exclusion criteria from the Geospatial Land Availability for Energy Systems (GLAES) model [26] for land eligibility analysis. The detailed list of exclusions and buffer distances is provided in Table C 1 in Supplementary Material.

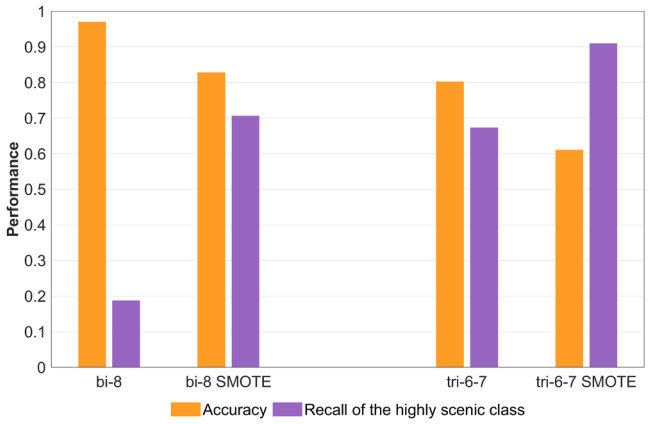

Fig. 3. Two examples (bi-8 and tri-6–7) of the models' accuracy and scenic class recall before and after using SMOTE.

In the medium and high preservation scenarios, an additional 1.5 km buffer was applied around (highly) scenic landscapes to limit visual exposure beyond the immediate footprint of wind farms [61]. Once the ineligible areas were removed, a near-future turbine model (13 MW capacity, 130 m hub height) [62,63] is placed over the remaining available area with a minimum spacing requirement of 8 rotor diameters [64] (approximately 1.4 km).

For each scenario, we estimated the turbine technical potential and corresponding levelized cost of electricity (LCOE) using RESKit [27] that combines high-resolution wind resource data with land eligibility constraints, turbines specifications, and economic parameters. Specifically, we simulated individual turbine yields over 5 years from 2018 to 2023 using the fifth generation of European Center for Medium-Range Weather Forecasts reanalysis (ERA5) [65] wind speeds extrapolated from 100 m to hub height with the logarithmic law [66] together with a synthetic power curve calculated within RESKit for the adopted turbine configuration [27]. Loss factor of 0.96 and 0.9 were applied to the turbine capacity factors to account for downtime and wake effects, respectively [63]. LCOE calculations followed the built-in capital expenditure (CAPEX) calculation in RESKit, where the baseline CAPEX was determined as $€_{2025}$15.46 million, with an annual operational expenditure (OPEX) as 2.2% of CAPEX [2].

To compare scenarios, we constructed cost curves [66] by ranking each turbine in ascending LCOE (merit-order approach). These curves illustrate the cost as a function of cumulative generation potential, enabling assessment of trade-offs between scenic landscape preservation and wind power cost-efficiency. To differentiate between total and exploitable cumulative potentials, we further excluded already exploited sites using the existing turbine dataset [59], applying the same minimum spacing requirement of 1.4 km.

To examine the spatial implications of scenicness-based exclusions, turbine energy yields and LCOE were aggregated at three different scales: continental, national, and sub-national from Nomenclature of Territorial Units for Statistics (NUTS-3), using sum and production-weighted median, respectively. This analysis quantifies the impact of stricter scenic landscape constraints on both deployment opportunities and economic performance in different regions, providing a basis for evaluating policy trade-offs locally between minimizing visual landscape impacts and achieving cost-effective renewable energy expansion.

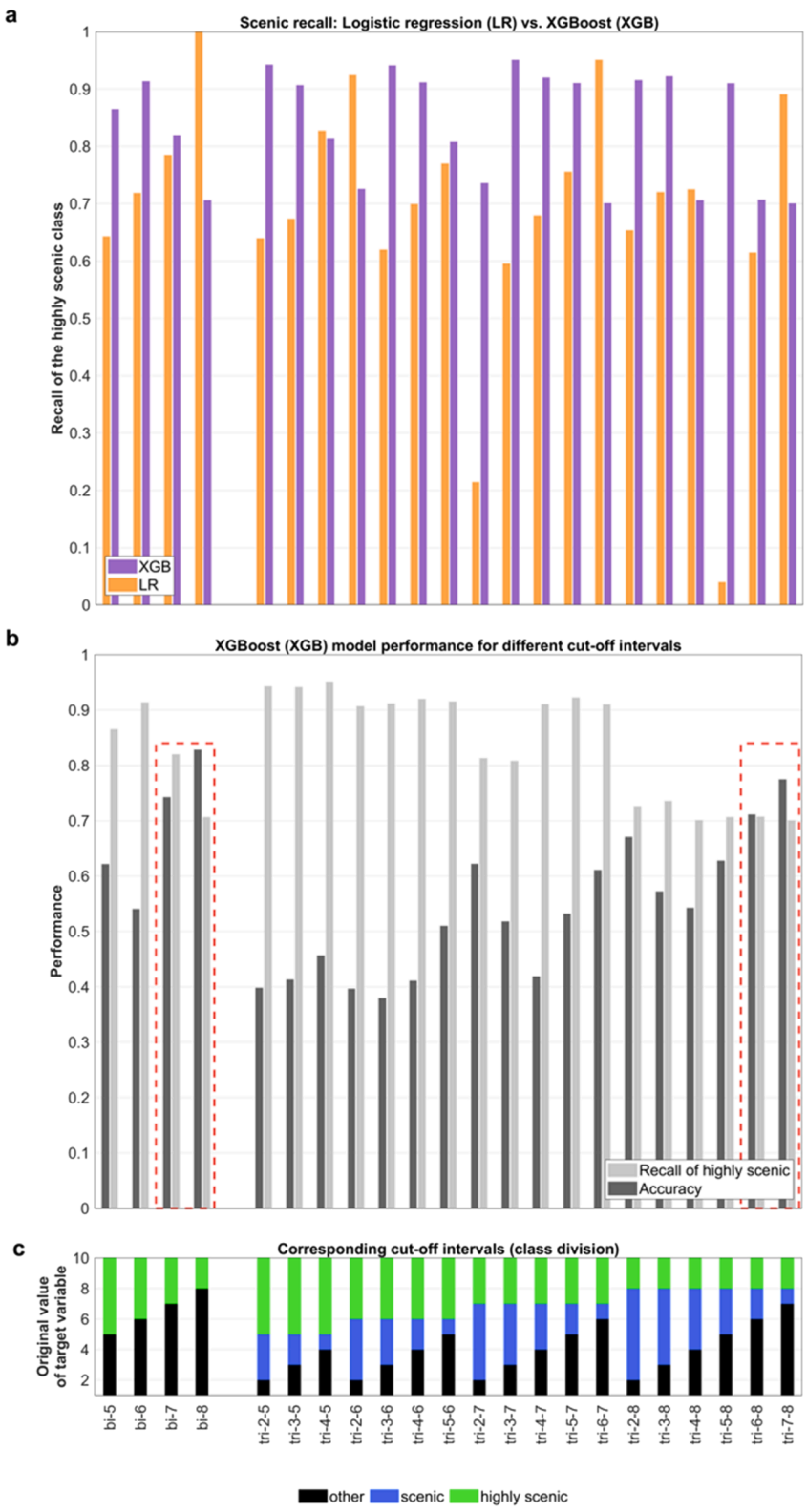

Fig. 4. (a) Model comparison – Logistic regression vs. XGBoost classifier on the recall of the highly scenic class for each target split; (b) Model performance (accuracy and highly scenic class recall) (c) for different cut-off intervals (class division) of the target variable. Highlighted in red are the models selected for further analysis.

3. Results

3.1. Model performance and validation

As mentioned in Section 2.3, prior to training, oversampling (SMOTE) was used to potentially improve the underrepresentation of the scenic class. To have a holistic view of the overall model performance, both scenic class recall and accuracy were used to examine the effect of using SMOTE. We found for both binary and ternary example targets (see Fig. 3), a significant increase of 80% on average in the recall

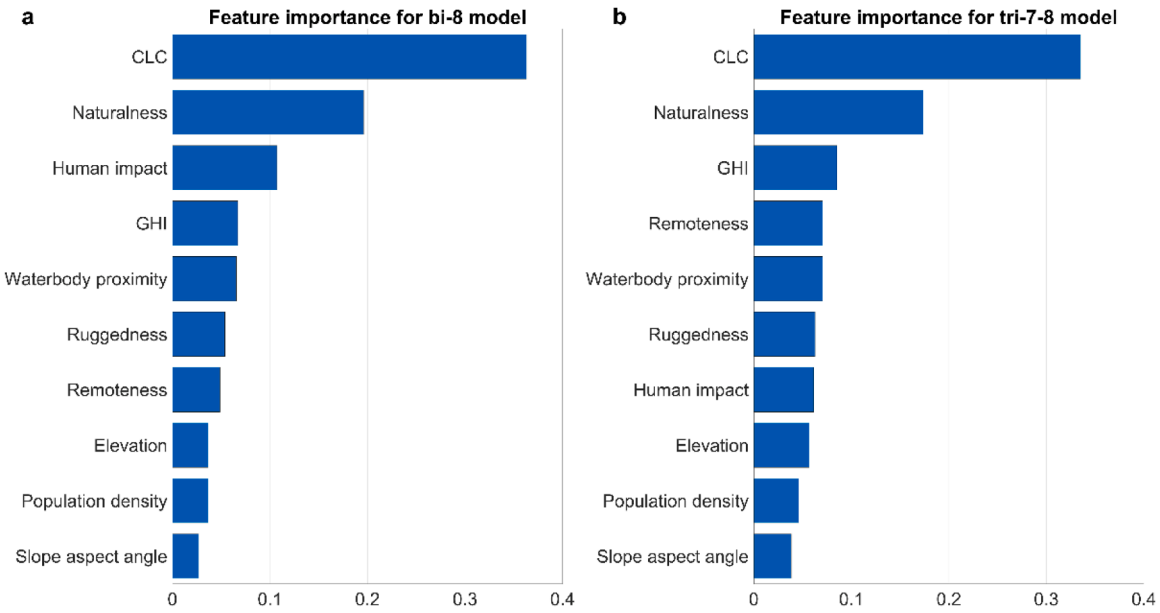

Fig. 5. Feature importance of the best-performing binary ("bi-8″) and best-performing ternary ("tri-7–8″) model. The numbers in the model names ("8″ and "7–8") are the used thresholds for class split of scenicness ratings from 1 (low) to 10 (high), as shown in Fig. 4c. The two abbreviations stand for CORINE Land Cover (CLC) and global horizontal irradiance (GHI), respectively.

of the highly scenic class can be observed after applying SMOTE, but it comes with a compromise in accuracy with an average 20% decrease.

For benchmarking, the same classification targets were trained with both LR and XGB models to compare the recall of the highly scenic class. Across all targets, XGB consistently outperformed LR during initial testing (see Fig. 4a). In contrast, two LR models exhibited convergence issues, resulting in near-zero recall values. Therefore, XGB was selected as the primary algorithm for subsequent analyses.

After applying SMOTE to address class imbalance, the performance of the XGB models was evaluated across all targets (Fig. 4b) based on point-level predictions on the test set prior to rasterization. Each target represents a specific threshold or set of thresholds used to separate the highly scenic class from less scenic ones (binary) or to include an additional scenic class (ternary). As shown, stricter cut-off intervals, corresponding to a smaller share of highly scenic samples, achieved higher overall accuracy (up to 82% for binary and 77% for ternary targets) but at the cost of reduced recall for the highly scenic class. Four models trained on targets "bi-7″, "bi-8″, "tri-6–8″, and "tri-7–8" (highlighted in Fig. 4b) were selected for further comparison, as they provided the best balance between the two metrics. Since only models with high cutoff thresholds could distinguish the classes with satisfactory performance, the class labels were adapted to reflect these thresholds: *highly scenic* and *other* for binary models, and *highly scenic, scenic*, and *other* for ternary ones.

To assess model generalizability to a different country, the four selected models were validated using an independent scenicness dataset for Germany [22]. The highest consistency levels, 93% for the binary case and 80% for the ternary case, were achieved by the "bi-8″ and "tri-7–8" models, respectively. Hence, these two models were selected as the final configurations for prediction landscape scenicness across Europe. Unlike the GB dataset, which includes at least one geotagged photograph for nearly every square kilometer grid cell, the German dataset is based on a smaller number of reference landscapes with photographic input and public votes, which were subsequently extrapolated to national coverage through regression. Despite these methodological differences, the strong agreement provides supporting evidence for the model's robustness and transferability. However, this should be interpreted with caution given the limited geographic scope of the training data.

Additionally, we assessed the impact of the post-processing smoothing step on the final 1 km^2 raster predictions in GB (see Table B 4 in Supplementary Materials). Smoothing improved the recall of the highly scenic class by an average of 18% at the expense of a reduction in overall accuracy by 5%. This increased the spatial extent of scenic classes by reducing isolated predictions, with around 5% of the predictions shifting from "other" to "scenic" or "highly scenic".

To better understand the determinants of model predictions, feature importance was analyzed for the two final models (see Fig. 5a,b). Among the input features, CLC categories, naturalness, GHI, and proximity to inland waterbodies were consistently ranked as the most influential predictors for landscape scenicness, with CLC and naturalness standing out ahead of others. Human impact contributed more strongly to the binary classification model (bi-8), while remoteness played a greater role in the ternary one (tri-7–8). Population density and slope aspect angle showed only marginal effects on the final classifications.

3.2. *Scenicness prediction across europe*

For the trained models to generalize predictions across Europe, the four landscape wilderness indicators: naturalness, ruggedness, remoteness, and human impact [24], were calculated at a continental scale for the first time (see Fig. 6a-d). These indicators respectively characterize landscape natural quality, terrain complexity, accessibility, and infrastructure density, providing valuable insights for large-scale landscape studies and sustainable energy planning. Distinct spatial patterns can be observed: highly natural areas are concentrated in Norway, the Alps, and northern Scotland, while the most rugged terrains are predominantly found in the Alpine region. The Nordic countries, particularly Norway, Sweden, and Finland, exhibit the lowest density of infrastructure, with their northern regions being among Europe's most remote areas.

Using these indicators along with six additional features, the final models predicted scenicness across EU25+4 in both binary and ternary form. The best-performing models classify 17–24% of Europe as *highly scenic*, up to 14% as *scenic*, and 69–76% as *other* (see Fig. 7a-d). Prominent clusters of (highly) scenic landscapes emerge in remote areas in northern and southern Europe, the Alps, and the highlands in northern Scotland, while the rest are dispersed across different regions. The

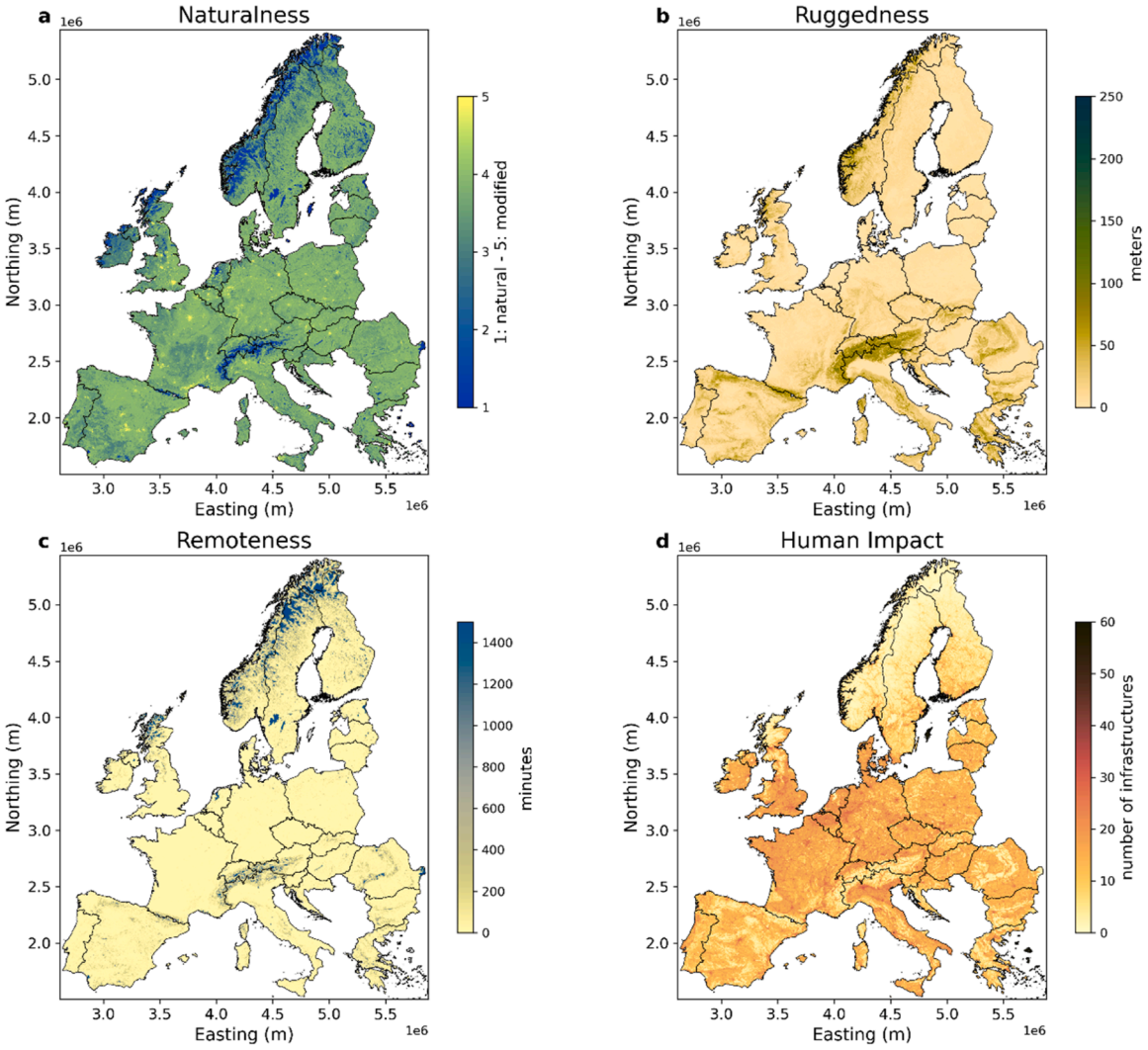

Fig. 6. Spatial distribution of the four wilderness indicators across EU25+4: (a) Naturalness (1: natural – 5: modified), (b) Ruggedness, (c) Remoteness, (d) Human Impact. EU25+4 is the EU27 excluding Malta and Cyprus but including the United Kingdom, Norway, Switzerland, and Liechtenstein.

models tend to classify coastal and mountainous regions as scenic, particularly in the United Kingdom, Norway, Spain, and Portugal. Similar land covers can be found in these regions, such as bare rocks and sparsely vegetated areas, indicating high naturalness.

Importantly, within highly scenic landscapes, a non-negligible share of land is technically eligible for wind deployment, 38% and 42% under binary and ternary classification, respectively (see Fig. 7c,d). This overlap between high scenic quality and technical feasibility highlights the potential land-use conflict and risk of social opposition. Spatial patterns of existing wind turbines [59] provide additional context: approximately 80% of wind turbines in EU25+4 are located in areas classified as *other*, where the median wind speed at 100 m above ground is 6.5 m/s. The remaining 20%, sited in (highly) scenic areas, exhibit a slightly higher median wind speed of 6.75 m/s. This distribution suggests that wind deployment tends to occur more frequently in less scenic areas, despite comparable or even superior wind resources in scenic regions. While this pattern is consistent with the model outputs, it should be interpreted as indicative rather than confirmatory, as turbine siting is shaped by regulatory, environmental, and other land-use constraints that may coincide with scenic landscapes.

By producing the first Europe-wide scenicness dataset, this study enables future research and planning exercises that address the trade-off between scenic landscape protection and renewable energy expansion in greater details. Beyond the energy sector, the dataset could support studies on ecosystem service valuation [67], tourism planning [68], or health [69] and well-being [70] links to natural beauty.

3.3. Impact of landscape preservation on onshore wind potentials

To analyze the trade-off between wind power cost-efficiency and scenic landscape preservation, we developed three exclusion scenarios based on the ternary scenicness classification. Across the EU25+4 region, which covers 4,730,631 square kilometers of land, the available area for onshore wind development under each scenario assessed using the geospatial land availability for energy systems (GLAES) framework [26] for land eligibility analyses is as follows:

- **Low preservation** (no exclusion of any scenic areas): 64.80% of land excluded
- **Medium preservation** (excluding “highly scenic” areas): 71.32% of land excluded
- **High preservation** (excluding both “highly scenic” and “scenic” areas): 79.89% of land excluded

The low preservation scenario yields results in line with previous studies [26,66,71], which estimated 23% to 40% of eligible land for onshore wind development in Europe. Using renewable energy simulation toolkit (RESKit) [27], we place turbines within eligible areas while

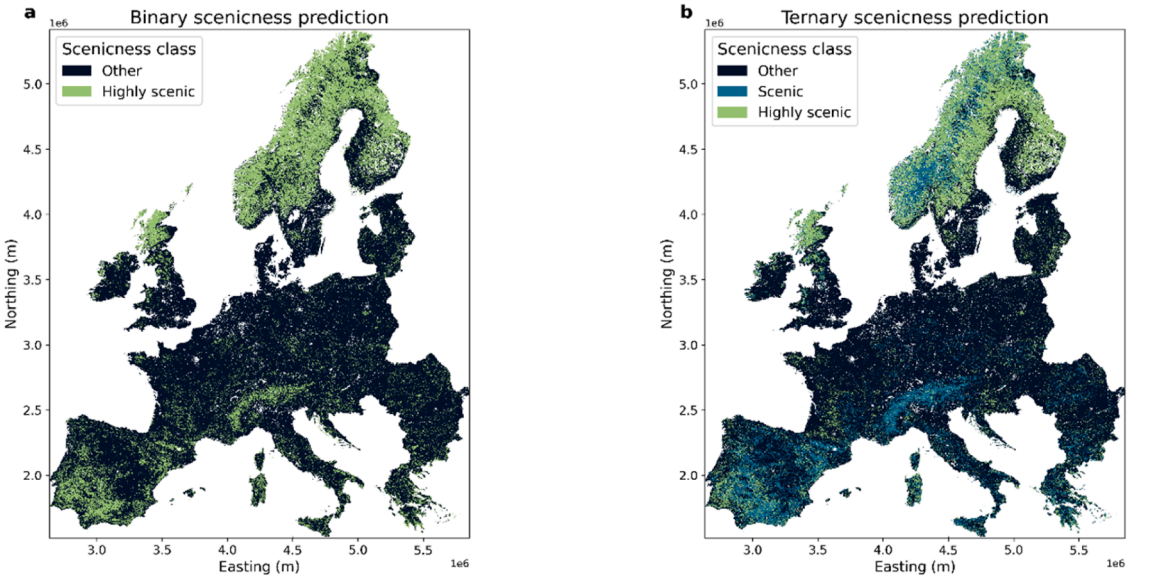

c Binary scenicness statistics

Class	Other	Highly Scenic
Total Area (km²)	3.44×10^6	1.08×10^6
Area (%)	76.1	23.9
Eligible Area for Wind (%)	28.4	38.2

d Ternary scenicness statistics

Class	Other	Scenic	Highly Scenic
Total Area (km²)	3.10×10^6	6.45×10^5	7.73×10^5
Area (%)	68.6	14.3	17.1
Eligible Area for Wind (%)	28.0	31.6	41.6

Fig. 7. Final predictions for landscape scenicness in EU25+4 excluding inland waterbodies and urban clusters: (a) Binary (0: other, 1: highly scenic), (b) Ternary (0: other, 1: scenic, 2: highly scenic). Summary statistics for the (c) binary and (d) ternary predictions include total area, percentage of land area, and percentage of area eligible for wind deployment within each scenicness class. EU25+4 is the EU27 excluding Malta and Cyprus but including the United Kingdom, Norway, Switzerland, and Liechtenstein.

enforcing minimum spacing requirement, and calculate both the annual energy yield and the (LCOE at the turbine level for each scenario, accounting for existing turbine locations.

Across scenarios, a clear trend of declining cumulative generation potential can be observed as landscape preservation becomes more stringent (see Fig. 8a-c). However, the magnitude of reduction varies significantly by country. Among the three current leading wind energy producers in Europe, Spain sees the largest drop, approximately 60%, in total generation potential from the low to the high preservation scenario. More significant decreases can be seen in other countries such as Norway, Switzerland, and Finland (see Table C 2 in Supplementary Material). In contrast, Germany experiences less than 10% reduction, suggesting its wind-suitable areas are less affected by scenic exclusions. The United Kingdom, while having the most favorable cost levels due to good wind resources in eligible areas, shows an intermediate reduction of around 30%. While Germany leads in wind power exploitation, having already developed 20% of its technically feasible sites, all three countries still retain substantial untapped potential. Notably, the gap between total and exploitable potential for Spain narrows with stricter landscape protection, suggesting that a considerable number of past deployments are located in (highly) scenic areas, pointing to potentially lower resistance.

At the European scale (EU25+4), we estimate a total annual onshore wind generation potential of approximately 26 PWh under the low preservation scenario, with about 3% of possible sites already exploited (see Fig. 8d). In the high preservation scenario, total generation potential decreases by 43%, reflecting substantial land exclusion. Notably, the aggregated cost curves steepen significantly under this scenario, indicating a faster rise in LCOE as the most cost-effective sites become exhausted.

Despite steeper cost curves under stricter landscape preservation, the median LCOE across EU25+4 remains relatively stable: from 54.1 €$_{2025}$/MWh in the high preservation scenario to 57.4 €$_{2025}$/MWh in the low one. This reflects the heterogeneous spatial relationship between scenicness and wind resource quality across Europe. Excluding scenic areas does not systematically remove the lowest-cost sites, and the remaining eligible locations can still exhibit competitive LCOE. However, this aggregate stability masks considerable spatial variation both within and across scenarios. Particularly in the low preservation scenario, significant differences in national median LCOE are observed, where Ireland exhibits the lowest production-weighted median LCOE of 33.8 €$_{2025}$/MWh and Slovenia shows the highest value of 111.5 €$_{2025}$/MWh, reflecting the variations in wind resource quality (see Table C 2 in Supplementary Material).

The variations in median LCOE across scenarios are more pronounced at the subnational (NUTS-3) level (cf. Fig. 9a,c). In mountainous regions such as the Alps and Norway, where scenic landscapes coincide with high-quality wind resources, stricter landscape preservation policies result in the loss of prime sites, driving a sharp increase in LCOE. By contrast, in countries like Sweden, Finland, Spain, and Portugal, regional median LCOEs remain stable across scenarios. However, these countries still experience substantial reductions in total generation potential (cf. Fig. 9b,d), indicating that, while the retained sites are still cost-effective, significant generation is foregone due to scenic area exclusions. Notably, the countries with highest total potential shift from France, Sweden, and Spain to France, Poland, and Germany, with the imposition of stricter scenic landscape protection. These findings underscore the importance of spatially explicit analysis: while Europe-wide medians may suggest resilience to stricter landscape protection, regional planning decisions require nuanced understanding of localized trade-offs between cost, potential, and preservation priorities.

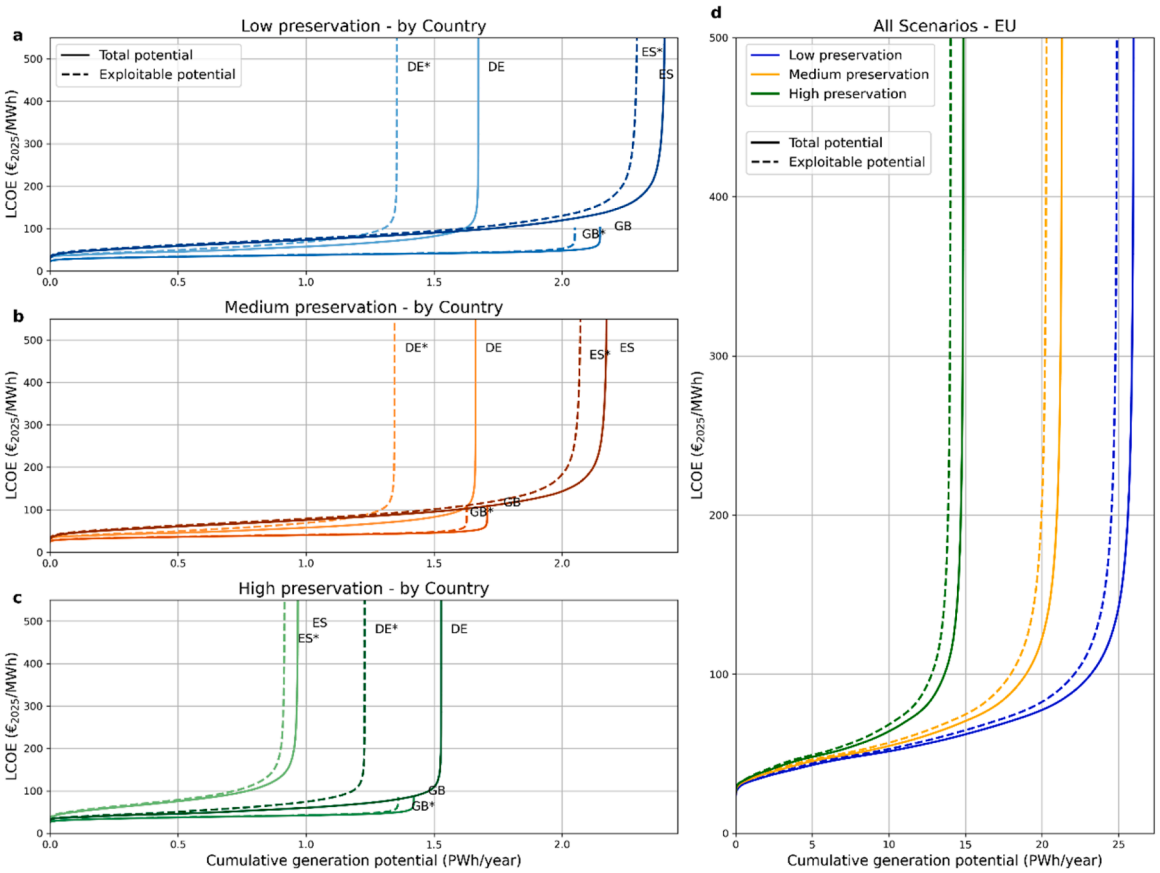

Fig. 8. Cost curves based on levelized cost of electricity (LCOE) of onshore wind energy for total potentials (solid line) and exploitable potentials (dashed line with asterisked label) after excluding location of existing turbines in top three countries (DE: Germany, GB: the United Kingdom, ES: Spain) in terms of existing wind capacity with (a) low landscape preservation, (b) medium landscape preservation, (c) high landscape preservation. The darker shade indicates the leading country in total potentials. (d) shows the total and exploitable potentials in all EU25+4 countries for the three landscape preservation scenarios.

4. Discussion

4.1. Model performance and feature interpretation

This study presents one of the first continental-scale predictions of landscape scenicness at high resolution, integrating four newly calculated wilderness indicators (naturalness, ruggedness, remoteness, and human impact) with other spatial features to train an ML model. These indicators, produced consistently for the EU25+4 region, not only supported the prediction task but also present valuable datasets for broader applications, such as grid connection cost estimation [14] with remoteness and footprint calculations [72] with human impact. The resulting scenicness dataset can be integrated into energy system optimization models to represent social acceptance factors in infrastructure siting decisions, enabling the assessment of trade-offs between cost, resource availability, and societal impacts [15].

Our models' predictions showed good alignment with the landscape value study in Germany [24], resulting from feature similarity. Their overall consistent feature importance rankings highlight a stable set of predictors that underpin public perceptions of scenicness [73]. CLC and naturalness emerged as the dominant predictors, with global horizontal irradiance and proximity to inland waterbodies following. The particularly high importance of CLC underscores the centrality of land cover composition and structure in shaping perceived visual quality, a pattern well-established in visual preference literature where natural and open landscapes are consistently preferred over urbanized areas [12,74].

Our results strongly support this pattern, where glaciers and perpetual snow, sparsely vegetated areas, and bare rocks are most often predicted as highly scenic, while non-irrigated arable land and urban fabric dominate in the lowest class. However, the model's GB-based training data introduces geographic bias, particularly due to the underrepresentation of Mediterranean land cover types such as vineyards, olive groves, and sclerophyllous vegetation (see Figure A 4 in Supplementary Material). This is further supported by the comparison of feature distributions between GB and the rest of Europe using summary statistics and Jensen-Shannon divergence (JSD), which is a symmetric and bounded measure of dissimilarity between two probability distributions [75,76] (see Table A 5 in Supplementary Material). The results show a moderate divergence in the most influential feature CLC (JSD = 0.15), with approximately 6% of European land cover classes not represented in the GB training data. Additional domain shifts are observed for two less important features, GHI and elevation, reflecting climatic and topographic characteristics absent in GB. However, most other features exhibit negligible divergence (JSD $<$ 0.03) and limited extrapolation beyond the GB range, suggesting the overall similarity of feature distributions at the continental scale. Expanding the training data with more crowd-sourced scenicness ratings on geotagged photographs from other countries, especially the Mediterranean region, and additional data sources that may serve as proxies would improve the model's transferability to more diverse landscape contexts.

Despite the overall similarity of feature importance between the models, differences in middle-ranking variables are observed. Specifically, remoteness is weighted more heavily in the ternary model (see Fig. 5a,b), helping resolve the additional "scenic" class. This is evident in the Alps (see Fig. 7a,b), which are classified as highly scenic in the binary model but downgraded in the ternary model due to relatively lower remoteness compared to northern Europe above 65°N (see Fig. 6c) that stays highly scenic across models. Such findings highlight how model

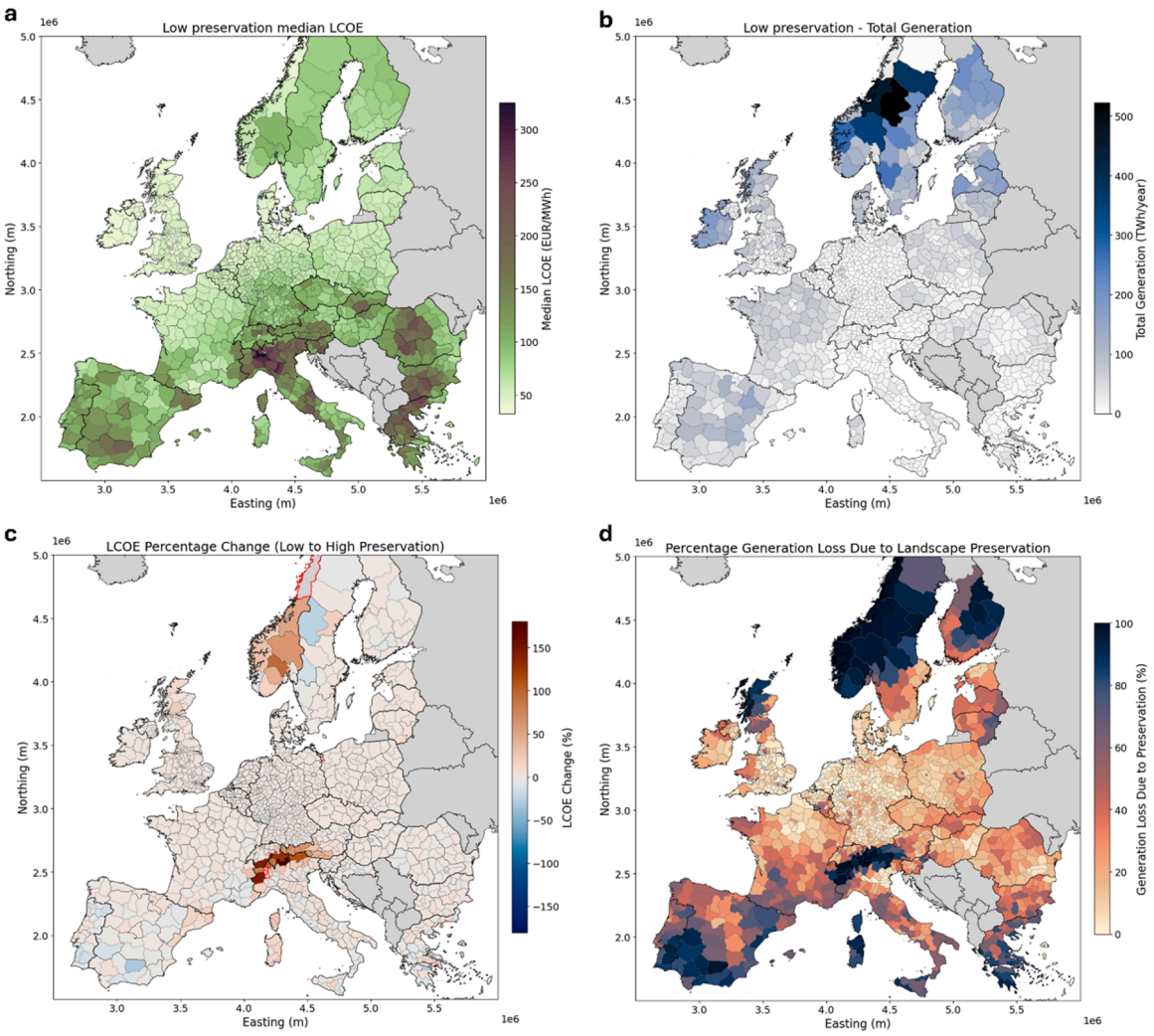

Fig. 9. (a) Map of NUTS3 level production-weighted mean levelized cost of electricity (LCOE) for the low preservation scenario, (b) total generation in TWh/year for each NUTS3 region, (c) change in production-weighted LCOE on NUTS3 level from the low preservation to the high preservation scenarios, (d) percentage loss in generation for each region when moving from low to high preservation. Note that in (c), 6 NUTS3 regions do not have any turbine placements in the high preservation scenario and are plotted as grey with red borders.

granularity can influence the contribution of individual predictors when capturing more nuanced distinctions [77].

Utilizing a variety of features increases the model complexity and assists in model behaviour explanation. For instance, while high naturalness and ruggedness frequently lead to highly scenic predictions, they alone do not guarantee such predictions when coupled with low remoteness, as seen in the developed parts of the Alps. Such multi-dimensionality underscores the benefit of using diverse indicators. Future work could extend this approach by incorporating seasonal dynamics [78] (e.g., vegetation changes) and cultural features [79] (e.g., heritage sites) to better capture context-dependent aspects of scenicness.

4.2. Implication of scenicness-aware resource assessment

The integration of scenicness predictions into wind resource assessment reveals important spatial trade-offs between cost-efficiency and landscape preservation. While Europe-wide median LCOEs remain relatively stable across preservation scenarios, this aggregate stability masks large subnational disparities. In mountainous regions (e.g., the Alps and Norway), excluding highly scenic areas, which often correspond to windy conditions, drive costs up. In contrast, flat terrain regions (e.g., Denmark and northern France) experience negligible cost changes due to more homogeneous distribution of wind resources [80]. These findings align with national case studies, which report similar patterns in Scottish Highlands [10,14] and in Germany [15,17]. In short, visual quality and wind resource quality are largely independent at continental scale, but regional overlaps can be significant.

Despite the stable median LCOE in most subnational regions, generation losses are substantial when scenic areas are excluded, potentially constraining national capacity expansion. The shift in main onshore wind electricity producers in Europe across preservation scenarios demonstrates that scenic landscape preservation efforts can alter the European wind energy supply geography. However, the fact that most countries have exploited few technically feasible sites indicates substantial expansion efforts needed for the energy transition.

From a policy perspective, these results stress the need for spatially explicit, multi-criteria planning. National-level medians risk obscuring localized hotspots where trade-offs between scenicness and wind resource are most acute. In practice, countries with low aggregate cost impacts (e.g., Germany) could still face localized opposition if projects are sited in valued scenic landscapes [81]. In others (e.g., Norway), where large shares of technical potential occur in scenic areas, mitigation strategies, such as micro-siting [82], turbine design adaptation [83], or co-locating with existing infrastructure [84], will be essential to reconcile deployment with public preferences.

The results also speak to debates on technology assumptions in long-

term potential modelling. We applied a near-future 13 MW turbine model [62] consistent with projected industry trend by 2040, acknowledging the long lead times of wind projects [63], which can exceed a decade. Using a single turbine configuration across all sites, however, overlooks local variations in wind regime and may misrepresent site-specific yields. Likewise, unaccounted infrastructure constraints (e.g., grid connection costs) could risk overestimating the attractiveness of remote sites that would require costly transport and grid extensions. Although a more computationally expensive assessment with site-specific turbine optimization and infrastructure modelling would yield greater local accuracy, our approach focuses on identifying national and subnational shifts relevant for continental planning.

5. Conclusion

This study developed a framework to predict landscape scenicness across Europe with machine learning and integrate these results into a continental-scale onshore wind resource assessment. By combining crowd-sourced scenicness ratings with geospatial indicators, the analysis provides one of the first quantitative evaluations of trade-offs between landscape preservation and renewable energy deployment.

Across the EU25+4 region, around one-fifth of land was classified as highly scenic, with considerable overlap between scenic areas and technically feasible sites for wind power. Scenario analysis revealed that stricter landscape preservation can reduce total onshore wind potential by up to 43%, yet with limited effect on Europe-wide median generation costs. However, subnational results showed that, in mountainous and coastal areas, scenicness exclusions remove prime wind sites and increased costs locally, while flatter regions remained largely unaffected. These findings underscore the need for spatially explicit planning that integrate social dimensions alongside techno-economic factors.

The model demonstrates promising performance across countries but remains constrained by training data limited to Great Britain, which may introduce geographic and demographic bias. Expanding the dataset to cover more diverse landscapes and incorporating additional contextual features would further enhance its transferability.

The produced scenicness and wilderness indicators constitute a useful dataset for future applications in energy planning, ecosystem service assessment, and tourism research. Integrating such perceptual and environmental dimensions into spatial energy models contributes to an energy transition that is not only low-carbon and cost-effective, but also culturally and aesthetically sustainable.

Declaration of generative AI and AI-assisted technologies in the manuscript preparation process

During the preparation of this work, the authors used ChatGPT in order to polish the language. After using this tool, the authors reviewed and edited the content as needed and take full responsibility for the content of the published article.

CRediT authorship contribution statement

Ruihong Chen: Writing – review & editing, Writing – original draft, Visualization, Methodology, Formal analysis, Conceptualization. **Tristan Pelser:** Writing – review & editing, Writing – original draft, Visualization, Methodology, Formal analysis. **Alena Lohrmann:** Writing – review & editing, Visualization, Supervision, Methodology. **Jann Michael Weinand:** Writing – review & editing, Supervision, Methodology. **Russell McKenna:** Writing – review & editing, Supervision, Methodology, Conceptualization.

Declaration of competing interest

The authors declare that they have no known competing financial interests or personal relationships that could have appeared to influence the work reported in this paper.

Acknowledgments

R. C., A. L., and R. M. gratefully acknowledged the financial support from the WIMBY project, funded by the Swiss State Secretariat for Education, Research, and Innovation (SERI) under the Swiss Federal Funding Programme for Horizon Europe under the grant agreement No. 101083460. T. P. and J. M. W. gratefully acknowledge the support from the Helmholtz Association as part of the program "Energy System Design".

Supplementary materials

Supplementary material associated with this article can be found, in the online version, at doi:10.1016/j.egyai.2026.100752.

Data availability•

The European scenicness predictions and four wilderness indicators in raster format generated in this study are openly available on Zenodo at https://doi.org/10.5281/zenodo.19682105 [85]. The Python code used for data processing and modelling are available from the corresponding author upon reasonable request.

References

[1] IEA, World Energy Outlook 2024. Paris: International Energy Agency; 2024. https://www.iea.org/reports/world-energy-outlook-2024 (accessed June 3, 2025).
[2] Stehly T, Duffy P, Hernando DM. Cost of wind energy review: 2024 edition. National Renewable Energy Laboratory (NREL); 2024. https://doi.org/10.2172/2479271.
[3] IRENA. Future of wind: deployment, investment, technology, grid integration and socio-economic aspects (A global energy transformation paper). Abu Dhabi: International Renewable Energy Agency; 2019. https://www.irena.org/publications/2019/Oct/Future-of-wind (accessed July 29, 2025).
[4] Intergovernmental Panel on Climate Change (IPCC). Climate change 2022 - Mitigation of climate change: working group iii contribution to the sixth assessment report of the intergovernmental panel on climate change. Cambridge: Cambridge University Press; 2023. https://doi.org/10.1017/9781009157926.
[5] McKenna R, Lilliestam J, Heinrichs HU, Weinand J, Schmidt J, Staffell I, Hahmann AN, Burgherr P, Burdack A, Bucha M, Chen R, Klingler M, Lehmann P, Lowitzsch J, Novo R, Price J, Sacchi R, Scherhaufer P, Schöll EM, Visconti P, Velasco-Herrejón P, Zeyringer M, Camargo LRamirez. System impacts of wind energy developments: key research challenges and opportunities. Joule 2025;9:101799. https://doi.org/10.1016/j.joule.2024.11.016.
[6] McKenna R, Pfenninger S, Heinrichs H, Schmidt J, Staffell I, Bauer C, Gruber K, Hahmann AN, Jansen M, Klingler M, Landwehr N, Larsén XG, Lilliestam J, Pickering B, Robinius M, Tröndle T, Turkovska O, Wehrle S, Weinand JM, Wohland J. High-resolution large-scale onshore wind energy assessments: A review of potential definitions, methodologies and future research needs. Renew Energy 2022;182:659–84. https://doi.org/10.1016/j.renene.2021.10.027.
[7] Tsani T, Weinand JM, Linßen J, Stolten D. Quantifying social factors for onshore wind planning – A systematic review. Renew Sustain Energy Rev 2024;203:114762. https://doi.org/10.1016/j.rser.2024.114762.
[8] Department for Energy Security and Net Zero, Renewable Energy Planning Data (REPD). UK Government; 2024. https://www.gov.uk/government/collections/renewable-energy-planning-data (accessed February 27, 2025).
[9] Lindvall D. Why municipalities reject wind power: A study on municipal acceptance and rejection of wind power instalments in Sweden. Energy Policy 2023;180:113664. https://doi.org/10.1016/j.enpol.2023.113664.
[10] McKenna R, Mulalic I, Soutar I, Weinand JM, Price J, Petrović S, Mainzer K. Exploring trade-offs between landscape impact, land use and resource quality for onshore variable renewable energy: an application to Great Britain. Energy 2022;250:123754. https://doi.org/10.1016/j.energy.2022.123754.
[11] Molnarova K, Sklenicka P, Stiborek J, Svobodova K, Salek M, Brabec E. Visual preferences for wind turbines: location, numbers and respondent characteristics. Appl Energy 2012;92:269–78. https://doi.org/10.1016/j.apenergy.2011.11.001.
[12] Spielhofer R, Thrash T, Hayek UW, Grêt-Regamey A, Salak B, Grübel J, Schinazi VR. Physiological and behavioral reactions to renewable energy systems in various landscape types. Renew Sustain Energy Rev 2021;135:110410. https://doi.org/10.1016/j.rser.2020.110410.
[13] Spielhofer R, Hunziker M, Kienast F, Hayek UWissen, Grêt-Regamey A. Does rated visual landscape quality match visual features? An analysis for renewable energy landscapes. Landsc Urban Plan 2021;209:104000. https://doi.org/10.1016/j.landurbplan.2020.104000.

[14] McKenna R, Weinand JM, Mulalic I, Petrović S, Mainzer K, Preis T, Moat HS. Scenicness assessment of onshore wind sites with geotagged photographs and impacts on approval and cost-efficiency. Nat Energy 2021;6:663–72. https://doi.org/10.1038/s41560-021-00842-5.

[15] Tsani T, Pelser T, Ioannidis R, Maier R, Chen R, Risch S, Kullmann F, McKenna R, Stolten D, Weinand JM. Quantifying the trade-offs between renewable energy visibility and system costs. Nat Commun 2025;16:3853. https://doi.org/10.1038/s41467-025-59029-1.

[16] Weinand JM, McKenna R, Kleinebrahm M, Scheller F, Fichtner W. The impact of public acceptance on cost efficiency and environmental sustainability in decentralized energy systems. Patterns 2021;2:100301. https://doi.org/10.1016/j.patter.2021.100301.

[17] Weinand JM, McKenna R, Heinrichs H, Roth M, Stolten D, Fichtner W. Exploring the trilemma of cost-efficiency, landscape impact and regional equality in onshore wind expansion planning. Adv Appl Energy 2022;7:100102. https://doi.org/10.1016/j.adapen.2022.100102.

[18] Price J, Mainzer K, Petrović S, Zeyringer M, McKenna R. The implications of landscape visual impact on future highly renewable power systems: A case study for Great Britain. IEEE Trans Power Syst 2022;37:3311–20. https://doi.org/10.1109/TPWRS.2020.2992061.

[19] European Commission (EC). Communication from the commission to the European Parliament, the Council, the European Economic and Social Committee of the regions - European wind power action plan, COM(2023) 669 final. Brussels: European Commission; 2023. https://eur-lex.europa.eu/legal-content/EN/TXT/?uri=CELEX:52023DC0669 (accessed July 29, 2025).

[20] Seresinhe CI, Preis T, Moat HS. Using deep learning to quantify the beauty of outdoor places. R Soc Open Sci 2017;4:170170. https://doi.org/10.1098/rsos.170170.

[21] Seresinhe CI, Moat HS, Preis T. Quantifying scenic areas using crowdsourced data. Environment and Planning B: Urban Analytics and City Science 2018;45:567–82. https://doi.org/10.1177/0265813516687302.

[22] Roth M, Hildebrandt S, Röhner S, Tilk C, Schwarzer von Raumer H-G, Roser F, Borsdorff M. Landscape as an area as perceived by people: empirically-based nationwide modelling of scenic landscape quality in germany. JoDLA 2018;3:129–37. https://doi.org/10.14627/537642014.

[23] Gobster PH, Nassauer JI, Daniel TC, Fry G. The shared landscape: what does aesthetics have to do with ecology? Landscape Ecol 2007;22:959–72. https://doi.org/10.1007/s10980-007-9110-x.

[24] Radford SL, Senn J, Kienast F. Indicator-based assessment of wilderness quality in mountain landscapes. Ecol Indic 2019;97:438–46. https://doi.org/10.1016/j.ecolind.2018.09.054.

[25] ScenicOrNot. ScenicOrNot: rate Great Britain's pretty places. University of Warwick Data Science Lab; 2015. https://scenicornot.datasciencelab.co.uk/ (accessed August 29, 2024).

[26] Ryberg DS, Tulemat Z, Stolten D, Robinius M. Uniformly constrained land eligibility for onshore European wind power. Renew Energy 2020;146:921–31. https://doi.org/10.1016/j.renene.2019.06.127.

[27] Ryberg DS, Caglayan DG, Schmitt S, Linßen J, Stolten D, Robinius M. The future of European onshore wind energy potential: detailed distribution and simulation of advanced turbine designs. Energy 2019;182:1222–38. https://doi.org/10.1016/j.energy.2019.06.052.

[28] Daniel TC. Whither scenic beauty? Visual landscape quality assessment in the 21st century. Landsc Urban Plan 2001;54:267–81. https://doi.org/10.1016/S0169-2046(01)00141-4.

[29] Scannell L, Gifford R. Defining place attachment: A tripartite organizing framework. J Environ Psychol 2010;30:1–10. https://doi.org/10.1016/j.jenvp.2009.09.006.

[30] Williams DR, Vaske JJ. The measurement of place attachment: validity and generalizability of a psychometric approach. Forest Sci 2003;49:830–40. https://doi.org/10.1093/forestscience/49.6.830.

[31] Lewicka M. Place attachment: how far have we come in the last 40 years? J Environ Psychol 2011;31:207–30. https://doi.org/10.1016/j.jenvp.2010.10.001.

[32] Bishop CM. Pattern recognition and machine learning. 1st ed. New York: Springer; 2006. https://link.springer.com/book/9780387310732 (accessed December 5, 2024).

[33] Kumar A, Goel S, Sinha N, Bhardwaj A. A review on unbalanced data classification. In: Uddin MS, Jamwal PK, Bansal JC, editors. Proceedings of International Joint Conference on Advances in Computational Intelligence. Algorithms for Intelligent Systems. Singapore: Springer Nature; 2022. p. 197–208. https://doi.org/10.1007/978-981-19-0332-8_14.

[34] He H, Garcia EA. Learning from imbalanced data. IEEE Trans Knowl Data Eng 2009;21:1263–84. https://doi.org/10.1109/TKDE.2008.239.

[35] European Environment Agency (EEA), CORINE Land Cover 2018 (raster 100m), Europe, 6-yearly - version 2020_20u1. Copernicus Land Monitoring Service; 2020. doi: 10.2909/960998c1-1870-4e82-8051-6485205ebbac (accessed December 1, 2024).

[36] European Space Agency (ESA), Copernicus Digital Elevation Model (GLO-90). Copernicus Programme; 2024. doi: 10.5270/ESA-c5d3d65 (accessed December 1, 2024).

[37] Ryberg D.S., Stolten D., Robinius M. The PRIOR datasets for rapid geospatial land eligibility analyses in Europe (V1). Mendeley Data 2020. doi:10.17632/trvfb3nwt2.1 (accessed December 1, 2024).

[38] World Bank Group, Global Solar Atlas 2.0. Solargis s.r.o. with funding provided by the Energy Sector Management Assistance Program (ESMAP); 2019. https://globalsolaratlas.info (accessed December 1, 2024).

[39] Pfeifroth, U., Kothe, S., Müller, R., Trentmann, J., Hollmann, R., Fuchs, P., Werscheck, M. Surface radiation data set - Heliosat (SARAH) - Edition 2. Satellite Application Facility on Climate Monitoring (CM SAF); 2019. doi: 10.5676/EUM_SAF_CM/SARAH/V002_01 (accessed December 1, 2024).

[40] Schiavina M., Freire S., Carioli A., MacManus K. GHS-POP R2023A - GHS population grid multitemporal (1975-2030). European Commission, Joint Research Centre 2026. doi:10.2905/2FF68A52-5B5B-4A22-8F40-C41DA8332CFE (accessed December 1, 2024).

[41] OpenStreetMap contributors, OpenStreetMap data. OpenStreetMap Foundation. https://www.openstreetmap.org (accessed December 1, 2024).

[42] Bentley JL. Multidimensional binary search trees used for associative searching. Commun. ACM 1975;18:509–17. https://doi.org/10.1145/361002.361007.

[43] Bresenham JE. Algorithm for computer control of a digital plotter. IBM Syst J 1965;4:25–30. https://doi.org/10.1147/sj.41.0025.

[44] K. Ward, N. Snoberger, U.-F. Service, Assessment of landscape scenic quality in The Angelina National Forest, Texas using gis and high-resolution digital imagery, (2009).

[45] White EM, Leefers LA. Influence of natural amenities on residential property values in a rural setting. Soc Nat Resour 2007;20:659–67. https://doi.org/10.1080/08941920601171998.

[46] Bishop ID, Hulse DW. Prediction of scenic beauty using mapped data and geographic information systems. Landsc Urban Plan 1994;30:59–70. https://doi.org/10.1016/0169-2046(94)90067-1.

[47] Yang J, El-Kassaby YA, Guan W. The effect of slope aspect on vegetation attributes in a mountainous dry valley, Southwest China. Sci Rep 2020;10:16465. https://doi.org/10.1038/s41598-020-73496-0.

[48] Tabassum-Abbasi MPremalatha, Abbasi T, Abbasi SA. Wind energy: increasing deployment, rising environmental concerns. Renew Sustain Energy Rev 2014;31:270–88. https://doi.org/10.1016/j.rser.2013.11.019.

[49] European Commission, Eurostat (GISCO), Urban clusters 2011 - raster dataset. 2022. https://ec.europa.eu/eurostat/web/gisco/geodata/population-distribution/clusters (accessed December 18, 2024).

[50] Chen T, Guestrin C. XGBoost: A scalable tree boosting system. In: Proceedings of the 22nd ACM SIGKDD International Conference on Knowledge Discovery and Data Mining. New York, NY, USA: Association for Computing Machinery; 2016. p. 785–94. https://doi.org/10.1145/2939672.2939785.

[51] Chawla NV, Japkowicz N, Kotcz A. Editorial: special issue on learning from imbalanced data sets. SIGKDD Explor Newsl 2004;6:1–6. https://doi.org/10.1145/1007730.1007733.

[52] Correcting for the effects of class imbalance improves the performance of machine-learning based species distribution models. Ecol Modell 2023;483:110414. https://doi.org/10.1016/j.ecolmodel.2023.110414.

[53] Friedman JH. Greedy function approximation: A gradient boosting machine. Ann Stat 2001;29:1189–232. https://doi.org/10.1214/aos/1013203451.

[54] Hastie T, Tibshirani R, Friedman J. Boosting and additive trees. In: Hastie T, Tibshirani R, Friedman J, editors. The elements of statistical learning: data mining, inference, and prediction. New York, NY: Springer; 2009. p. 337–87. https://doi.org/10.1007/978-0-387-84858-7_10.

[55] Moran PAP. Notes on continuous stochastic phenomena. Biometrika 1950;37:17–23. https://doi.org/10.2307/2332142.

[56] Fortin M-J, Dale MRT. Spatial analysis: a guide for ecologists. Cambridge: Cambridge University Press; 2005. https://doi.org/10.1017/CBO9780511542039.

[57] Mulugeta G, Zewotir T, Tegegne AS, Juhar LH, Muleta MB. Classification of imbalanced data using machine learning algorithms to predict the risk of renal graft failures in Ethiopia. BMC Med Inform Decis Mak 2023;23:98. https://doi.org/10.1186/s12911-023-02185-5.

[58] Chawla NV, Bowyer KW, Hall LO, Kegelmeyer WP. SMOTE: synthetic minority over-sampling technique. J Artif Intell Res 2002;16:321–57. https://doi.org/10.1613/jair.953.

[59] Hahmann AN, Davis N, Alonso-De-Linaje NG, Floors R. Wind in my backyard (WIMBY) Deliverable 1.2 - Wind resources API (b). Wind in my backyard (WIMBY) project; 2024. https://wimby.eu/resource/d1-2-wind-resources-api-b/ (accessed July 22, 2025).

[60] van Zanten BT, Van Berkel DB, Meentemeyer RK, Smith JW, Tieskens KF, Verburg PH. Continental-scale quantification of landscape values using social media data. Proc Natl Acad Sci 2016;113:12974–9. https://doi.org/10.1073/pnas.1614158113.

[61] Guo W, Wenz L, Auffhammer M. The visual effect of wind turbines on property values is small and diminishing in space and time. Proc Natl Acad Sci 2024;121:e2309372121. https://doi.org/10.1073/pnas.2309372121.

[62] Wiser R, Rand J, Seel J, Beiter P, Baker E, Lantz E, Gilman P. Expert elicitation survey predicts 37% to 49% declines in wind energy costs by 2050. Nat Energy 2021;6:555–65. https://doi.org/10.1038/s41560-021-00810-z.

[63] Pelser T, Weinand JM, Kuckertz P, McKenna R, Linssen J, Stolten D. Reviewing accuracy & reproducibility of large-scale wind resource assessments. Adv Appl Energy 2024;13:100158. https://doi.org/10.1016/j.adapen.2023.100158.

[64] Pelser T, Weinand JM, Kuckertz P, Stolten D. ETHOS.REFLOW: an open-source workflow for reproducible renewable energy potential assessments. Patterns 2025;6:101172. https://doi.org/10.1016/j.patter.2025.101172.

[65] Hersbach H., Bell B., Berrisford P., Biavati G., Horányi A., Muñoz Sabater J., Nicolas J., Peubey C., Radu R., Rozum I., Schepers D., Simmons A., Soci C., Dee D., Thépaut J.-N. ERA5 hourly data on single levels from 1940 to present. Copernicus Climate Change Service (C3S) Climate Data Store (CDS); 2023. doi: 10.24381/cds.adbb2d47 (accessed June 20, 2025).

[66] McKenna R, Hollnaicher S, Ostman v. d. Leye P, Fichtner W. Cost-potentials for large onshore wind turbines in Europe. Energy 2015;83:217–29. https://doi.org/10.1016/j.energy.2015.02.016.
[67] Smardon R. Ecosystem Services for scenic quality landscape management: A review. Land (Basel) 2021;10:1123. https://doi.org/10.3390/land10111123.
[68] Bachi L, Ribeiro SC, Hermes J, Saadi A. Cultural Ecosystem Services (CES) in landscapes with a tourist vocation: mapping and modeling the physical landscape components that bring benefits to people in a mountain tourist destination in southeastern Brazil. Tour Manag 2020;77:104017. https://doi.org/10.1016/j.tourman.2019.104017.
[69] Seresinhe CI, Preis T, Moat HS. Quantifying the impact of scenic environments on health. Sci Rep 2015;5:16899. https://doi.org/10.1038/srep16899.
[70] Seresinhe CI, Preis T, MacKerron G, Moat HS. Happiness is greater in more scenic locations. Sci Rep 2019;9:4498. https://doi.org/10.1038/s41598-019-40854-6.
[71] Eurek K, Sullivan P, Gleason M, Hettinger D, Heimiller D, Lopez A. An improved global wind resource estimate for integrated assessment models. Energy Econ 2017;64:552–67. https://doi.org/10.1016/j.eneco.2016.11.015.
[72] Venter O, Sanderson EW, Magrach A, Allan JR, Beher J, Jones KR, Possingham HP, Laurance WF, Wood P, Fekete BM, Levy MA, Watson JEM. Sixteen years of change in the global terrestrial human footprint and implications for biodiversity conservation. Nat Commun 2016;7:12558. https://doi.org/10.1038/ncomms12558.
[73] Fisher A, Rudin C, Dominici F. All models are wrong, but many are useful: learning a variable's importance by studying an entire class of prediction models simultaneously. J Mach Learn Res 2019;20:1–81.
[74] Franěk M. Landscape preference: the role of attractiveness and spatial openness of the environment. Behav Sci (Basel) 2023;13:666. https://doi.org/10.3390/bs13080666.
[75] Lin J. Divergence measures based on the Shannon entropy. IEEE Trans Inf Theory 1991;37:145–51. https://doi.org/10.1109/18.61115.
[76] Nguyen H-V, Vreeken J. Non-parametric Jensen-Shannon divergence. In: Appice A, Rodrigues PP, Costa VSantos, Gama J, Jorge A, Soares C, editors. Machine learning and knowledge discovery in databases. Cham: Springer International Publishing; 2015. p. 173–89. https://doi.org/10.1007/978-3-319-23525-7_11.
[77] Kuhn M, Johnson K. Nonlinear classification models. In: Kuhn M, Johnson K, editors. Applied predictive modeling. New York, NY: Springer; 2013. p. 329–67. https://doi.org/10.1007/978-1-4614-6849-3_13.
[78] Półrolniczak M, Kolendowicz L. The effect of seasonality and weather conditions on human perception of the urban–rural transitional landscape. Sci Rep 2023;13:15047. https://doi.org/10.1038/s41598-023-42014-3.
[79] Khaledi HJ, Khakzand M, Faizi M. Landscape and perception: A systematic review. Landsc Online 2022:97, 1098. https://doi.org/10.3097/LO.2022.1098.
[80] Davis NN, Badger J, Hahmann AN, Hansen BO, Mortensen NG, Kelly M, Larsén XG, Olsen BT, Floors R, Lizcano G, Casso P, Lacave O, Bosch A, Bauwens I, Knight OJ, van Loon AP, Fox R, Parvanyan T, Hansen SBK, Heathfield D, Onninen M, Drummond R. The Global wind Atlas: A high-resolution dataset of climatologies and associated web-based application. Bulletin of the American Meteorological Society 2023;104(8):E1507–25. https://doi.org/10.1175/BAMS-D-21-0075.1.
[81] Kraft P, Kraft B. Public attitudes and the socio-political divide surrounding onshore wind power in Norway. Front Sustain Energy Policy 2025;4:1538828. https://doi.org/10.3389/fsuep.2025.1538828.
[82] Hanssen F, May R, Nygård T. High-resolution modeling of uplift landscapes can inform micrositing of wind turbines for soaring raptors. Environ Manage 2020;66:319–32. https://doi.org/10.1007/s00267-020-01318-0.
[83] May R, Nygård T, Falkdalen U, Åström J, Hamre Ø, Stokke BG. Paint it black: efficacy of increased wind turbine rotor blade visibility to reduce avian fatalities. Ecol Evol 2020;10:8927–35. https://doi.org/10.1002/ece3.6592.
[84] Harold J, Bertsch V, Lawrence T, Hall M. Drivers of people's preferences for spatial proximity to energy infrastructure technologies: A cross-country analysis. EJ 2021;42(4):47–90. https://doi.org/10.5547/01956574.42.4.jhar.
[85] Chen R, Lohrmann A, McKenna R. European landscape scenicness predictions and wilderness indicators (2.0) [dataset]. Zenodo; 2026. https://doi.org/10.5281/zenodo.19682105.